NARROW-BAND UV RADIATION (250–260 nm) FROM INTRACAVITY DOUBLING A SINGLE-MODE RING DYE LASER

C.R. WEBSTER, L. WÖSTE * and R.N. ZARE
Department of Chemistry, Stanford University, Stanford, CA 94305, USA

Received 27 August 1980

Generation of continuous-wave, tunable UV radiation (250–260 nm) by intracavity doubling a coumarin-515 ring dye laser is described. A cooled (200–280 K) ADP crystal with end faces cut at Brester's angle is placed inside the laser ring cavity which has been compensated for astigmatism and coma. UV output powers at 254 nm of 120 μW and 60 μW are achieved with the laser operating multimode (bandwidth $\simeq$ 20 GHz) and single-mode (bandwidth $\lesssim$ 50 MHz), respectively. Continuous single-mode scans over the 253.7 nm mercury profile demonstrate sub-Doppler resolution of the Hg 6s6p $^3P_1^o$ – $6s^2\ ^1S_0$ transition.

1. Introduction

Narrow-band tunable UV radiation for possible application to photochemical, analytical, and spectroscopic studies, has been generated from an intracavity-doubled cw ring dye laser. This work not only extends the wavelength range available from second harmonic generation (SHG) to 250 nm, but demonstrates that single-mode operation of ring lasers to produce very narrow ($\lesssim$ 100 MHz linewidth) tunable UV output is readily achieved.

The availablity of cw pump sources and stable dyes limits dye laser output to wavelengths above 320 nm. The production of tunable light in the deeper UV therefore requires the use of nonlinear optics such as harmonic generation and sum frequency mixing [1]. To date, these methods have provided the lowest wavelength UV radiation, but this has been accomplished using pulsed dye laser systems whose theoretical bandwidth is at best the Fourier transform limit of the laser pulse duration [2].

For narrower bandwidths cw operation is necessary. A cw dye laser system with intracavity second-harmonic generation was first described in 1972 by Gabel and Herscher [3]. In 1978 Wagstaff and Dunn [4] frequency doubled a rhodamine 6G single-mode ring laser using an ADA intracavity crystal to produce UV output in the range 292–302 nm with good output power and stability. More recently, Mariella [5] reached wavelengths near 247 nm by extracavity doubling a coumarin 480 linear dye laser to produce UV output with a bandwidth of about 2.5 GHz, while Clough and Johnston [6] reported intracavity doubling of a coumarin 535 linear dye laser to produce UV output with a bandwidth of about 4 GHz in the range 257–260 nm. The design which is described below takes advantage of the high circulating power inside a single-mode ring dye laser to generate UV output (250–260 nm) by intracavity frequency doubling. While the present laser system is free running ($\lesssim$50 MHz bandwidth), actively-stabilized (1 MHz bandwidth) single-mode cw ring lasers are commercially available, suggesting that cw UV radiation with very narrow bandwidths ($\sim$2 MHz) will be available in the near future.

2. The coumarin ring laser

The six-mirror cavity configuration, designed specifically for operation using coumarin 515 (coumarin 30) dye is illustrated in fig. 1. All mirrors are coated for high reflectivity (>99.8% at 507 nm) in the dye range of 485–550 nm for beams $\sim$15° from normal incidence. Gimble mirror mounts with micrometer ad-

* Present address: Ecole Polytechnique Federal de Lausanne, Department de Physique, 33 Ave. de Cour CH1007 Lausanne, Switzerland.

justment are fixed on aluminium blocks which define a beam level 12.5 cm above the supporting NRC optical table having pneumatic isolation mounts. Excitation of the dye is provided by a Spectra-Physics model 171 krypton ion laser which produces up to 3.6 W at 413 nm all lines. The ion laser output first has its linear polarization rotated by 90° to match the horizontally-polarized dye laser and is then focused by a 2.5 cm radius of curvature mirror into the vertical dye jet.

A 1×10^{-3} molar solution of coumarin 515 (Exciton) in ethylene glycol containing a few ml of cyclooctatetraene (COT) is used in a homebuilt dye nozzle/circulator system. The circulator is a water-cooled two-chamber design incorporating a 10 μm filter (Millipore), a 1/8 horse-power motor (GE), and magnetic coupling assembly (Micropump). A bypass valve allows the dye solution pressure behind the nozzle to be varied up to 100 PSIG. The nozzle is made by optically contacting two fused silica blocks (15 mm × 10 mm × 5 mm) at their largest surfaces and then separating these surfaces by precision polished fused silica spacers of ~250 μm thickness. The 15 mm long nozzle has, therefore, a rectangular cross-sectional area of ~5 mm × 250 μm. The dye jet is vertically mounted to cross the plane of the laser ring at 90°, exit through a clearance hole in the table and be gently collected to avoid acoustic feedback.

Kogelnik and co-workers [7] have described how the stability of a cw dye-laser cavity may be optimized by compensating astigmatic distortions introduced by focusing into Brewster elements with those introduced by off-axis mirrors. An improvement which also reduces losses due to comatic aberration was suggested by Johnston and Runge [8]. These results have been incorporated into the design of the cavity described here. Referring specifically to fig. 1, the angle $\alpha(\sim 4^\circ)$ is chosen according to the condition

$$R \sin(\alpha/2) \tan(\alpha/2) = Nt, \tag{1}$$

where R is the radius of curvature of mirrors R_1 and R_2, t is the dye-jet thickness and

$$N = [(n^2 - 1)/n^4]\,(n^2 + 1)^{1/2}, \tag{2}$$

where n is the refractive index of the dye solution ($n = 1.4$ for ethylene glycol).

A second beam waist occurs in the ring laser midway between mirrors R_3 and R_4 of radii of curvature equal to 50 cm. At this location is inserted the frequency-doubling unit, the optical assembly of an Inrad model 5-11 "supercooled" temperature phase-matching system. This unit contains an ADP crystal close to 5 cm long, and the heaters and sensors required to set the crystal temperature.

For the purpose of calculating the astigmatism resulting from focusing into the ADP crystal through the two (each direction) Brewster windows and balancing this with that resulting from the off-axis mirrors ($R_3 = R_4 = R = 50$ cm), we use an effective crystal

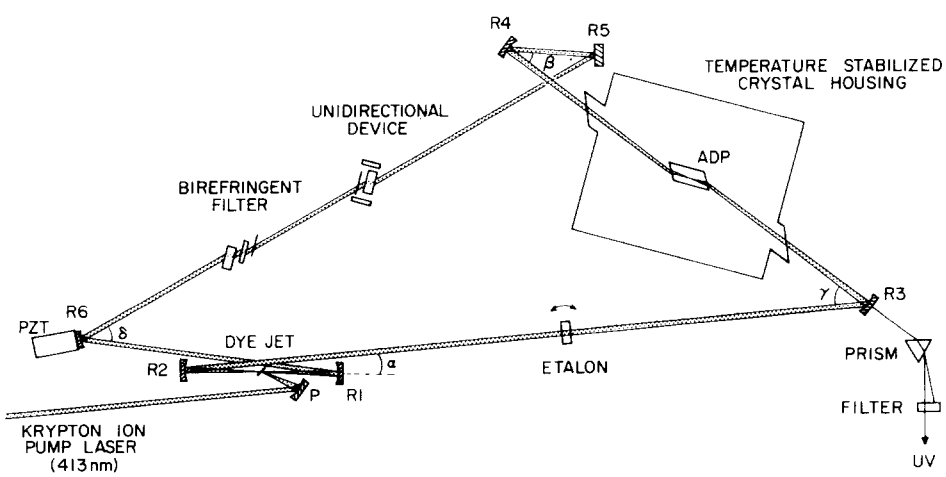

Fig. 1. Schematic of the coumarin ring laser: P = pump mirror; $\alpha \simeq 4^\circ$; $\beta \simeq 25^\circ$; $\gamma \simeq 34^\circ$; $\delta \simeq 42^\circ$; mirrors $R_1 = R_2 = 5$ cm, $R_3 = R_4 = 50$ cm, $R_5 = R_6 = \infty$; and PZT = piezoelectric translator.

thickness of 5.4 cm and $n = 1.52$. Then, according to (1) the angle at which astigmatic compensation is achieved is 12.5°. For our cavity design the large size of the doubling unit allows $\beta/2$ to be set to 12.5°, but restricts $\gamma/2$ to about 17°. However, the cavity is essentially astigmatically compensated. As demonstrated by Dunn and Ferguson [9], the Z-configuration and the crystal orientation used mean that coma and astigmatic compensation is possible both overall and at the focus.

In the ADP frequency doubling system described here the phase-matching condition is satisfied by 90° phase-matching [10], i.e. when the fundamental and harmonic beam propagate at an angle of 90° to the optical axis of the crystal. For a given wavelength, this is possible only over a small temperature range. Thus the tuning of the fundamental and hence the UV output wavelength must be accompanied by an appropriate change in crystal temperature, which is maintained at the set temperature to ±0.01 K. To generate UV in the range 250–260 nm the ADP crystal must be cooled to 200–280 K. During multimode operation, oscillation occurs simultaneously in both directions around the ring and UV radiation is coupled out via mirrors R_3 and R_4 (both having greater than 75% transmission in the range 250–260 nm). The longitudinal mode structure of the laser is monitored using a scanning Fabry-Perot interferometer (Spectra-Physics 470) with a 2 GHz free spectral range (FSR).

3. Single-mode operation

Only a single, uncoated etalon (thickness 6.35 mm, FSR ≃ 16.2 GHz) inserted into the ring is necessary to ensure single-mode operation. The optical bistability [4] is completely removed however by the insertion into the ring of a homebuilt unidirectional device (UDD).

The unidirectional device comprised a Faraday rotator and a polarization rotation plate [11,12] both at Brewster's angle. The angular rotation of the linearly polarized beam in the unfavored direction is 3.5° for each element.

The single-mode dye laser could be scanned either in a mode-hopping or a continuous-scan configuration. For the former scans, the etalon is rotated in the horizontal plane by a synchronous motor drive and the birefringent filter optimized during such a scan. In this way scans over ~1 cm^{-1} in the visible or ~2 cm^{-1} in the UV are readily achieved.

In the continuous scan configuration, the signal from a photodiode monitoring the visible light (the mirrors transmit 0.15% of the intracavity power) is fed into a Lansing model 80.215 lockin stabilizer consisting of a tuned amplifier, a reference channel, a phase-sensitive detector, an integrator, and a high-voltage dc amplifier. A small modulation voltage at 520 Hz from the stabilizer drives the piezoelectric translator (PZT) (Lansing model 21.938) supporting the cavity mirror R_6. The generated correction signal is also applied to this PZT and the cavity is thereby "locked" to the intracavity etalon. Thus, when the etalon is rotated by means of a synchronous motor, continuous single-mode scans are possible. The effective ring length in air is 0.84 m as determined by the measured cavity free spectral range (c/nL) of ≃ 120 MHz in the visible.

4. Laser performance

Efficient generation of UV radiation in the 255 nm range by frequency doubling a coumarin laser is more difficult than generating 295 nm radiation by frequency doubling a rhodamine-6G laser for three reasons: only a few (≤5) W pump power at 413 nm can be delivered by commercially-available krypton ion lasers; the efficiency of the dye is relatively poor, requiring the addition of COT to the dye solution; and coumarin 515 in ethylene glycol is photochemically unstable, degrading appreciably after tens of watt-hours excitation. In the simple ring arrangement shown in fig. 1 with the crystal, etalon and UDD absent, the laser could be tuned over the range 485–550 nm with a threshold at the peak of this emission requiring only a few hundred milliwatts pump power at 413 nm. (See table 1.) The whole doubling unit was measured to have an absorption at 514.4 nm of 4%, and insertion into the cavity raised the required pump power to 0.85 W for a fresh dye solution (1.4 W typically after ~10 hours operation). For a fixed crystal temperature of about 234 K, at 508 nm, tuning of the birefringent filter as measured by a spectrometer showed that the UV output had its half-intensity points at ±3 cm^{-1} in the visible corresponding to ±6 cm^{-1} in the UV.

Table 1

(A) Pump laser power at 413 nm required to reach the dye laser threshold of oscillation

Simple cavity	0.40 W
With doubling unit inserted	0.85 W
With UDD also inserted	1.30 W
With etalon also inserted	1.40 W

(B) Ring laser characteristics with 3.6 W pump power at at 413 nm

Tuning range	485–550 nm
Demonstrated UV tuning range	250–260 nm
Multimode operation:	
Intracavity power	5 W [a]
Generated UV power at 254 nm	120 ± 15 μW
Single-mode operation:	
Intracavity power at 508 nm	2 W
Generated UV power at 254 nm	60 ± 10 μW

[a] 2.5 W each direction

At 508 nm with the laser running multimode the UV output power at mirror R_3 is 60 ± 10 μW for an intracavity power of about 2.5 W in one direction. A similar output power is observed at mirror R_4, and therefore the multimode laser gives 120 μW UV power at 254 nm. It should be noted that following its emergence from the crystal the UV output must pass through, in each direction, 2 plates or 4 surfaces oriented at Brewster's angle for the opposite polarization, and a mirror only 86% transmitting. Therefore, a total of 200 μW UV power must emerge from the doubling crystal. When the unidirectional device and the etalon are inserted, the pump threshold is raised to 1.3 W, and 1.4 W, respectively, for a fresh dye solution. In this configuration the laser operated single-mode, producing 60 ± 10 μW UV output power at 254 nm for a 3.6 W pump power. With a 2.5 W pump power, single-mode operation is readily achieved over the range 500–520 nm corresponding to 250–260 nm UV output.

By comparing the generated UV power with the intracavity visible power given in table 1, a conversion coefficient $c \simeq 5 \times 10^{-5}$ W^{-1} is experimentally determined for the 90° phase-matched, 50 mm long ADP crystal. Since the absorption coefficient of the crystal used was not negligible it is expected that the conversion efficiency is reduced by thermal phase mismatching [13].

5. Fluorescence excitation spectrum of atomic mercury

To illustrate the capabilities of the present laser system, the fluorescence excitation spectrum was recorded of the 253.7 nm $^3P_1 - {}^1S_0$ transition of natural mercury (figs. 2–4). As shown in figs. 2 and 3 there are ten hyperfine lines, one from each of the five even-mass isotopes (196, 198, 200, 202, and 204), two from Hg-199 ($I = 1/2$) and three from Hg-201 ($I = 3/2$). The differing nuclei cause the lines to be displaced in frequency so that the spectrum under Doppler-limited resolution shows five distinct features (the "hand" of mercury). Because the Hg-196 isotope has a natural abundance of 0.146%, its presence does not contribute significantly to the observed pattern.

The fluorescence excitation spectrum of natural

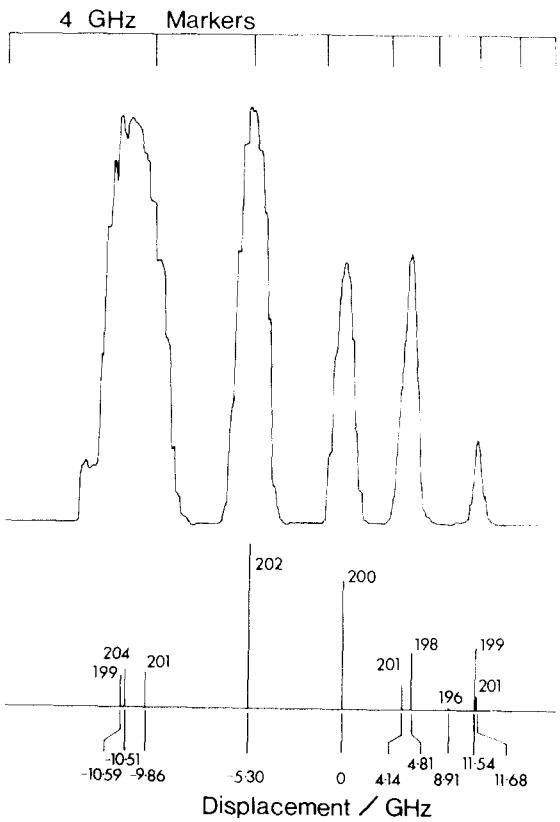

Fig. 2. The Doppler-limited fluorescence excitation spectrum of natural Hg vapor in a cell at 0°C. The measured displacements below are from Bitter [14], replotted on our frequency scale. The amplifier sensitivity was increased by × 2 after the Hg-200 peak.

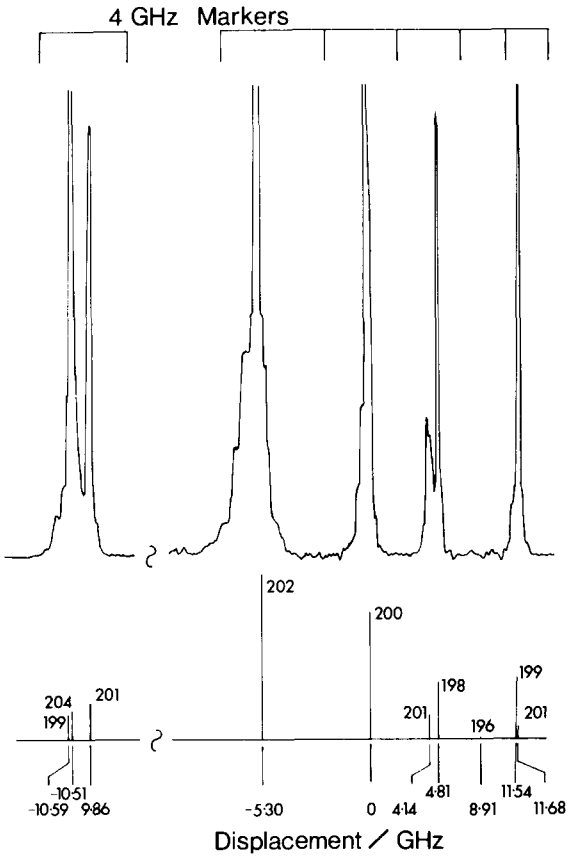

Fig. 3. The sub-Doppler fluorescence excitation spectrum of natural Hg in an atomic beam. Note the change in frequency scale between the first and last four components.

mercury in a bulb (fig. 2) and in a beam (fig. 3) is recorded by scanning the single-mode laser (with mode hopping) and detecting the resultant resonance fluorescence using a RCA 1P-28 phototube in conjuction with phase-sensitive discrimination (PAR Model 124A lockin). In between hyperfine components, scattered light from the cell was about three orders of magnitude lower than the fluorescence signal. The mode-hop positions, occuring every 240 MHz, can be clearly seen in these figures, causing a familiar histogram appearance. Note that the measured Doppler width of $\simeq 1.2$ GHz is in good agreement with that calculated.

In figs. 2 and 3 the frequency scales are nonlinear as a result of the angle tuning of the etalon. The UV power is also nonlinear. The visible intracavity power falls as the etalon is scanned away from normal, causing the UV output to drop quadratically with this change. In addition, the crystal temperature is not set for optimum phase-matching at the center of the line profile, causing the visible conversion efficiency to depend further on frequency. In both figs. 2 and 3 the UV power drops dramatically with increasing frequency; no correction was made for this variation.

The "bulb" and "beam" experiments are quite different. In the former, the mercury is contained in a quartz cell at a pressure of 2.3×10^{-4} torr, corresponding to 0°C. In the latter, UV output (divergence < 1 mrad) was passed vertically through a one-meter baffle arm where it intersected perpendicularly an atomic beam of mercury. The beam source comprised a double chamber stainless-steel oven mounted in a differentially-pumped adjoining chamber. Both chambers were evacuated by oil diffusion pumps and liquid-nitrogen-cooled surfaces. A typical mercury backing pressure of 50 torr was used behind the 0.2 mm diameter nozzle. The atomic beam was collimated by a cooled iris.

A comparison of figs. 2 and 3 shows that the latter has a marked increase in resolution resulting from the decreased effective Doppler width of the beam. Indeed, under beam conditions the linewidths are so narrow that it is possible to hop over a line in the mode-hopping scan of fig. 3. This explains the weak appearance of the Hg-201 component at +4.14 GHz. The underlying broader part of the lineshape (obvious for the Hg-202 line which is well off-scale in the figure) is the Doppler-limited contribution from background Hg (5×10^{-6} torr) in the beam apparatus.

Fig. 4 shows single-mode continuous scans over se-

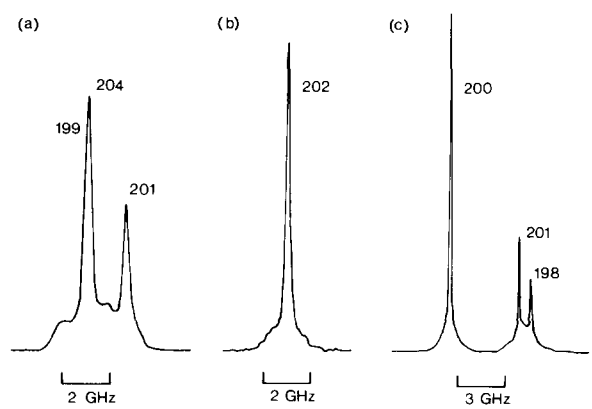

Fig. 4. Single mode continuous scans over selected hyperfine components of the Hg $^3P_1^o = {}^1S_0$ transition.

lected lines, where the resolution achieved, the linewidth, and the background emission contribution are all apparent. We found that the measured linewidth depended on the time taken to scan over a line, and was a convolution of the contributions from the laser bandwidth and the atomic beam/fluorescence collection geometry. For example, scanning over the Hg-202 line shown in fig. 4b took about 5 s and resulted in a measured linewidth of ~100 MHz (fwhm). Scans (a) and (c) were made over slightly longer and shorter times, respectively, (due to the nonlinearity of the etalon scan) and showed slightly larger and narrower linewidths, respectively. We conclude that the free running single-mode laser bandwidth was $\lesssim 50$ MHz (in the visible) over a period of several seconds. This figure is reasonable for a free-running dye laser using COT additive, no elements to reduce pressure fluctuations in the dye jet, and no 2 μm filter to remove microbubbles. The relative increase in bandwidth due to the modulation applied to the PZT was negligible.

6. Summary

An intracavity-doubled cw ring dye laser has been operated single-mode to wavelengths as short as 500 nm; the UV output at 254 nm was 60 ± 10 μW in a bandwidth of $\leqslant 100$ MHz (over a few seconds). The coumarin 515 dye laser has been tuned over the 253.7 nm mercury profile to illustrate sub-Doppler resolution and single-mode continuous scanning.

It is well known [15] that crystals with very low absorption and cavities with very low losses are necessary for high efficiency second harmonic generation. In the present laser system having a pump power of 3.5 W, the power in the single-mode ring cannot exceed ~1 W. In the future, it should be possible to reduce the present intracavity losses and to actively stabilize the cavity to $\simeq 2$ MHz UV bandwidth. Although the present laser system is designed to operate over 250–260 nm, this range can easily be extended to shorter or longer wavelengths by appropriate choice of dye mirror coatings, and crystal temperature. It is anticipated that the unique characteristics of this laser will be most effectively exploited in ultra high resolution spectroscopy using Doppler-free techniques.

Acknowledgement

Support by the National Science Foundation under NSF CHE 80-06524 is gratefully acknowledged.

References

[1] G.D. Boyd and D.A. Kleinman, J. Appl. Phys. 39 (1968) 3639;
S. Blit, E.G. Weaver, T.A. Rabson and F.K. Tittel, Appl. Optics 17 (1978) 721;
J. Paisner, M.L. Spaeth, D.C. Gerstenberger and I.W. Ruderman, Appl. Phys. Letters 32 (1978) 476.
[2] R. Wallenstein and T.W. Hänsch, Optics Comm. 14 (1975) 353.
[3] C. Gabel and M. Hercher, IEEE J. Quantum Electron. QE-8 (1972) 850.
[4] C.E. Wagstaff and M.H. Dunn, J. Phys. D: Appl. Phys. 12 (1979) 355.
[5] R.P. Mariella, J. Chem. Phys. 71 (1979) 94.
[6] P.N. Clough and J. Johnston, Chem. Phys. Letters 71 (1980) 253.
[7] H.W. Kogelnik, E.P. Ippen, A. Dienes and C.V. Shank, IEEE J. Quantum Electron. QE-8 (1972) 373.
[8] W.D. Johnston and P.K. Runge, IEEE J. Quantum Electron. QE-8 (1972) 724.
[9] M.H. Dunn and A.I. Ferguson, Optics Comm. 20 (1977) 214.
[10] R.C. Miller, G.D. Boyd and A. Savage, Appl. Phys. Letters 6 (1965) 77.
[11] P.W. Smith, IEEE J. Quantum Electron. QE-4 (1968) 485.
[12] S.M. Jarrett and J.F. Young, Laser Focus 14 (1978) 16.
[13] M. Okada and S. Ieiri, IEEE J. Quantum Electron. QE-7 (1970) 469.
[14] F. Bitter, Appl. Optics 1 (1962) 1.
[15] A.I. Ferguson and M.H. Dunn, IEEE J. Quantum Electron. QE-13 (1977) 751.